Accepted Manuscript

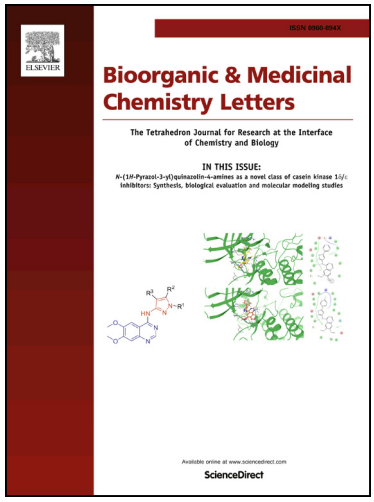

Novel 1,2-dihydroquinazolin-2-ones: Design, synthesis, and biological evaluation against *Trypanosoma brucei*

ThanhTruc Pham, Madeline Walden, Christopher Butler, Rosario Diaz-Gonzalez, Guiomar Pérez-Moreno, Gloria Ceballos-Pérez, Veronica Gomez-Pérez, Raquel García-Hernández, Henry Zecca, Emma Krakoff, Brian Kopec, Ogar Ichire, Caden Mackenzie, Marika Pitot, Luis Miguel Ruiz, Francisco Gamarro, Dolores González-Pacanowska, Miguel Navarro, Amy B. Dounay

PII: S0960-894X(17)30728-X
DOI: http://dx.doi.org/10.1016/j.bmcl.2017.07.032
Reference: BMCL 25145

To appear in: *Bioorganic & Medicinal Chemistry Letters*

Received Date: 8 June 2017
Accepted Date: 10 July 2017

Please cite this article as: Pham, T., Walden, M., Butler, C., Diaz-Gonzalez, R., Pérez-Moreno, G., Ceballos-Pérez, G., Gomez-Pérez, V., García-Hernández, R., Zecca, H., Krakoff, E., Kopec, B., Ichire, O., Mackenzie, C., Pitot, M., Ruiz, L.M., Gamarro, F., González-Pacanowska, D., Navarro, M., Dounay, A.B., Novel 1,2-dihydroquinazolin-2-ones: Design, synthesis, and biological evaluation against *Trypanosoma brucei*, *Bioorganic & Medicinal Chemistry Letters* (2017), doi: http://dx.doi.org/10.1016/j.bmcl.2017.07.032

Novel 1,2-dihydroquinazolin-2-ones: Design, synthesis, and biological evaluation against *Trypanosoma brucei*

ThanhTruc Pham,[a] Madeline Walden,[a] Christopher Butler,[a] Rosario Diaz-Gonzalez,[b] Guiomar Pérez-Moreno,[b] Gloria Ceballos-Pérez,[b] Veronica Gomez-Pérez[b], Raquel García-Hernández[b], Henry Zecca,[a] Emma Krakoff,[a] Brian Kopec,[a] Ogar Ichire,[a] Caden Mackenzie,[a] Marika Pitot,[a] Luis Miguel Ruiz,[b] Francisco Gamarro,[b] Dolores González-Pacanowska,[b] Miguel Navarro,[b] Amy B. Dounay[a*]

[a]*Colorado College, Department of Chemistry and Biochemistry, 14 E. Cache La Poudre, Colorado Springs, CO 80903*
[b]*Instituto de Parasitología y Biomedicina "López-Neyra" Consejo Superior de Investigaciones Científicas (CSIC), Granada 18100 Spain*

Abstract

In 2014, a published report of the high-throughput screen of >42,000 kinase inhibitors from GlaxoSmithKline against *T. brucei* identified 797 potent and selective hits. From this rich data set, we selected **NEU-0001101** (**1**) for hit-to-lead optimization. Through our preliminary compound synthesis and SAR studies, we have confirmed the previously reported activity of **1** in a *T. brucei* cell proliferation assay and have identified alternative groups to replace the pyridyl ring in **1**. Pyrazole **24** achieves improvements in both potency and lipophilicity relative to **1**, while also showing good in vitro metabolic stability. The SAR developed on **24** provides new directions for further optimization of this novel scaffold for anti-trypanosomal drug discovery.

African sleeping sickness, also known as human African trypanosomiasis (HAT), threatens millions of people in sub-Saharan Africa.[1] HAT is caused by the parasitic protozoa *Trypanosoma brucei*, which are transmitted to humans by the bite of the tsetse fly. More than 95% of HAT cases occur in western and central Africa and are caused by *T. b. gambiense*; the other HAT infections, in eastern and southern Africa, are caused by *T. b. rhodesiense.* The disease occurs in two stages and is fatal if left untreated. In the first stage, parasites proliferate in the hemolymphatic system, and symptoms are relatively non-specific, presenting a challenge for early diagnosis and intervention. In the second stage, parasitic invasion of the central nervous system (CNS) causes progressive neurological dysfunction, including convulsions, serious sleep disturbance, and ultimately coma and death.

Current treatments for Stage II HAT are inadequate due to their poor safety profiles, marginal efficacy, and complex dosing protocols.[2,3] Additionally, drug-resistant infections have emerged in recent years.[4] The World Health Organization has identified the complexity of current therapies as a major issue for sustaining ongoing disease control efforts.[5] A safe, orally

administered drug that is effective against both stages and strains of HAT could pave the way for elimination of the disease, a milestone that is within reach for the first time in history.[6]

To address the urgent need for new HAT medicines, a number of innovative new academic-industrial partnerships have emerged. In one recent collaborative effort, a high-throughput screen (HTS) of 42,444 kinase inhibitors from the GlaxoSmithKline (GSK) screening collection against *T. brucei* was completed.[7] This study identified 797 sub-micromolar *T. brucei* growth inhibitors that were also >100-fold selective over HepG2 cells. The publication of this rich HTS data set has provided researchers worldwide with an abundance of potential new starting points for HAT drug discovery programs. We reviewed this HTS data set with a goal of identifying a hit with attractive properties for development into an oral, brain-penetrant drug. To ensure that the data from our follow-up to the GSK HTS are readily available to the broader neglected disease research community, we report herein our progress on hit-to-lead development of one new series.

From the hundreds of hits identified in the GSK screen, we selected **NEU-0001101** (**1**, **Figure 1**) for hit-to-lead optimization. One attractive feature of **1** is its low molecular weight (299 g/mol). Typically, during the optimization of a hit into a clinical candidate, the compound's molecular weight increases. Therefore, selecting a low MW hit allows for increasing the molecular size without exceeding targeted CNS properties.[8,9] Additionally, **1** has only one hydrogen-bond donor (HBD). Minimizing the number of HBD groups in drug molecules also correlates with improved brain-penetration, a requisite property for any Stage II therapeutic.[7-10] The favorable MW and HBD, in addition to other calculated properties, contribute to the excellent CNS multi-parameter optimization (MPO) score (5.6/6.0) for **1**.[7-8] Additionally, the optimal ligand efficiency (LE)[11] range for hit compounds is 0.25-0.35.[12,13] With an LE = 0.37, **1** has excellent LE for a hit compound. Finally, synthetic tractability of a hit is a key consideration for enabling rapid hit-to-lead follow-up studies. Based on our preliminary analysis of the structure of **1**, we anticipated that synthesis of this hit and additional analogs in this series would be straightforward.

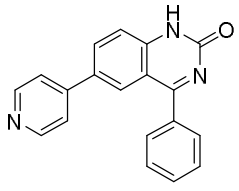

NEU-0001101 (1)
T. brucei (GSK) EC_{50} = 0.84μM
MW = 299
HBD = 1
CNS MPO = 5.6
LE = 0.37

Figure 1. Structure and key data for HTS hit **NEU-0001101** (**1**)

In order to initiate hit-to-lead medicinal chemistry studies, we devised a flexible, two-step synthesis of **1** from commercially available 2-amino-5-bromobenzonitrile (**2**, **Scheme 1**).[14] In the first step, phenylmagnesium bromide (R^1MgBr) addition to the nitrile followed by trapping of the Grignard adduct with methyl chloroformate afforded 6-bromo-4-phenylquinazolin-2(*1H*)-one (**3**). Whereas the previously reported protocol for this Grignard reaction used diethyl ether as solvent,[13] our use of THF improved both the yield and the safety profile for this step. Suzuki coupling of **3** with a variety of boronic acids under microwave conditions allows for readily diversifying this series via the R^2 substituent.[15] The simplicity and brevity of this modular synthetic approach has enabled the rapid synthesis of analogs (**4**) in this series.

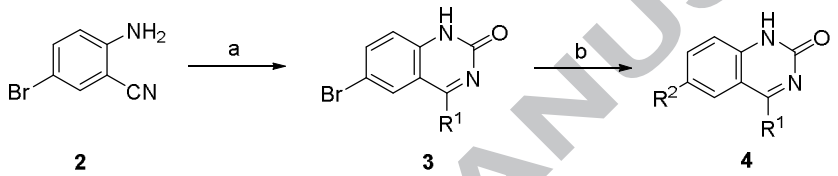

Scheme 1. General synthetic approach toward compounds **1 - 27**. a) R^1MgBr, THF; ClC(O)OMe (12 – 91% yield) b) $R^2B(OH)_2$, $Pd(PPh_3)_4$, Na_2CO_3, DMF/H_2O (10 – 89%).

Hit confirmation via resynthesis and retesting of the hit compound is a crucial first follow-up step for any hit-to-lead medicinal chemistry effort.[16-18] A new synthetic batch of **1** was prepared and showed an approximately 2-fold reduction in potency (EC_{50} = 1.89 μM) in our *T. brucei* cell proliferation assay compared to the initial GSK assay result (EC_{50} = 0.84 μM).[6] This minor shift may be attributed to a number of factors, including minor differences in the biological assay protocols, as well as differences in sample purity between the new batch of **1** compared to the original GSK sample collection batch. Despite the slight loss of potency in this retest, **1** remained an attractive compound for hit-to-lead optimization, due to its highly favorable drug-like physicochemical properties and good LE.

Following our hit confirmation studies, we initiated structure-activity relationship (SAR) exploration with a focus on modifying the pyridyl ring in **1**. Unsubstituted 4-pyridyl groups present a potential drug-drug interaction (DDI) risk.[19] Thus, preliminary SAR studies explored the effect of altering this pyridyl group, and all new analogs were evaluated in the *T. brucei* cell proliferation assay (Table 1).

Table 1. Effect of substituted pyridyl analogs on *T. brucei* growth inhibition and MRC5 cytotoxicity

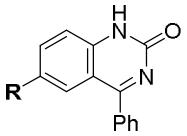

Cmpd.	R	*T. brucei* EC_{50} (μM)[a]	clogP[b]	*T. brucei* LLE[c]	MRC5 (μM)
1		1.89 ±0.09	3.35	2.38	>50
5		5.32 ±0.8	3.48	1.80	>50
6		5.35 ±0.5	3.35	1.93	>50
7	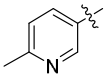	5.29 ±0.66	3.48	1.80	>50
8	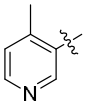	5.07 ±0.05	3.86	1.44	>50
9	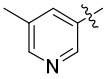	5.24 ±0.23	3.86	1.42	>50
10	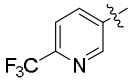	5.21 ±0.18	4.61	0.67	>50
11	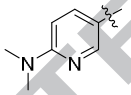	2.04 ±0.19	4.05	1.64	>50
12	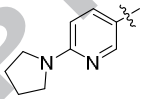	1.77 ±0.08	4.45	1.30	>50
13	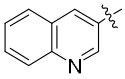	1.73 ±0.11	4.72	1.04	>50

[a] EC_{50} values are mean ± SD; n = 4 measurements; All SEM values are within 25%.
[b]Calculated partition coefficient;[29] [c](LLE = pEC_{50} – clogP)

These studies show that the addition of a methyl group (compound **5**) or the shift of the pyridyl nitrogen from the 4-pyridyl to 3-pyridyl (compounds **6** – **9**) result in a <3-fold loss of potency in the *T. brucei* assay. Furthermore, the addition of a flanking trifluoromethyl group (compound **10** vs. **6**) has no significant impact on potency. This suggests that a basic pyridyl nitrogen is not essential to this series, or that the increased lipophilic interactions of the trifluoromethyl group can offset the weakening of electrostatic interactions achieved through the weakly basic pyridine. Larger substituents on the pyridyl ring are also tolerated, with the largest groups (compounds **12** and **13**) achieving comparable potency to the original hit compound. However, it is important to note that the lipophilic ligand efficiency (LLE)[20,21] in this series erodes with the addition of these large, lipophilic substituents. Thus, from a standpoint of optimizing for LLE, compound **1** remains the best in this preliminary evaluation of the pyridyl group. Additionally, all new analogs in this series were tested in an MRC5 counterscreen to evaluate cytotoxicity in a human cell line. These compounds show no activity in the MRC5 cell proliferation assay, demonstrating that they are selective for *T. brucei* in their inhibition of cellular proliferation.

To further explore the importance of the pyridyl group for activity in this series, we synthesized a set of analogs in which the pyridyl ring was replaced by substituted phenyl groups (**Table 2**). Direct replacement of the pyridyl group in **1** with a phenyl group (compound **14**) causes a ~2.5-fold loss in potency. This result further demonstrates that the pyridine nitrogen may provide a modest potency boost, but it is not essential and can be replaced by other aromatic groups to improve the drug safety profile of this chemical series. The mono-fluorophenyl analogs (compounds **15** – **17**) all showed comparable potency (EC_{50} = 3.71 – 4.29 μM). The addition of the 4-cyano substituent (compound **18**) restored potency to match the original pyridyl hit (**1**), perhaps due to a favorable hydrogen bonding interaction. The addition of larger substituents on the phenyl group (compounds **19** – **21**) did not provide any significant changes in potency. In general, compounds **20** and **21**, combined with the previous data on compounds **11** and **12**, demonstrate that large substituents at the *para* position on this aromatic group are tolerated and potentially beneficial to potency in the *T. brucei* assay. Overall, the SAR for substitution of this phenyl group is relatively flat (EC_{50} range: 1.71 – 5.7 μM), and no dramatic potency improvements were achieved in this initial compound set. Evaluation of these compounds in the MRC5 assay further demonstrates the selectivity across this series for *T. brucei* antiproliferative activity over the human cell line.

Table 2. Effect of substituted phenyl analogs on *T. brucei* growth inhibition and MRC5 cytotoxicity

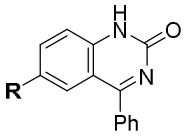

Cmpd.	R	*T. brucei* EC_{50} (μM)[a]	clogP[d]	*T. brucei* LLE[e]	MRC5 (μM)
14	Ph	4.88 ±0.58	4.56	0.75	>50
15	2-F-Ph	3.71 ±0.55	4.71	0.72	>50
16	3-F-Ph	4.29 ±0.29	4.71	0.66	>50
17	4-F-Ph	3.88 ±0.25	4.71	0.71	>50
18	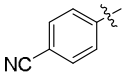	1.71 ±0.17	4.42	1.35	>50
19	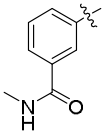	5.7 ±0.45[b]	3.64	1.61	>50
20	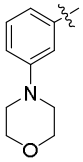	5.17 ±0.26[c]		0.83	>50
21	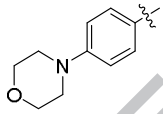	2.17 ±0.37	4.45	1.21	23.7

[a] EC_{50} values are mean ± SD; n = 4 measurements; All SEM values are within 25% unless otherwise noted.[b] SEM = 2.14;
[c] SEM = 1.84; [d]Calculated partition coefficient; [29] [e] (LLE = pEC_{50} – clogP)

Numerous analyses have demonstrated that highly lipophilic compounds experience a significant rate of attrition due to ADME problems and toxicity.[22-26] In an effort to reduce the lipophilicity and improve the LLE of molecules in this series, the replacement of the pyridyl group of **1** with alternative heteroaromatic groups was investigated (**Table 3**). Although replacement of the pyridyl group with a more polar and less basic pyrimidine (compound **22**) resulted in a significant potency loss, isoxazole and pyrazole groups were advantageous (compounds **23** – **27**). In particular, pyrazoles **24** and **25** show improved LLE relative to our hit compound **1** due to their improvements in both potency and cLogP. These improvements suggest that the pyrazole achieves useful, polar drug-target interactions. Notably, the *N*-methyl pyrazole **26** has 4- to 5-fold lower potency relative to pyrazoles **24** and **25**, suggesting that their

potency is enhanced by their hydrogen bond donating capability. Likewise, the weaker potency of *N*-methyl pyrazole **27** may be attributed to the absence of the hydrogen bond donor group or the conformational change in the biaryl group induced by the *N*-methyl group. Among the isomeric pyrazoles **24** and **25**, we have chosen to focus on **24** for further optimization, due to its higher selectivity for *T. brucei* over MRC5. A preliminary set of in vitro ADME assays confirms that **24** achieves a desirable lipophilicity ($LogD_{7.4}$ =2.2) and metabolic stability (HLM Cl_{int} = 19 μL/min/mg; Rat hepatocyte Cl_{int}<1 μL/min/10^6 cells). The modest aqueous solubility (8 μM) of **24** is one focus of ongoing efforts at further optimizing this series.

Table 3. Effect of pyrimidine, isoxazole, and pyrazole analogs on *T. brucei* growth inhibition and MRC5 cytotoxicity

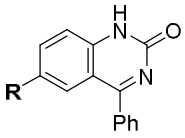

Cmpd.	R	*T. brucei* EC_{50} (μM)[a]	clogP[c]	*T. brucei* LLE[d]	MRC5 (μM)
22		10.04 ±2.95	2.64	2.36	>50
23		2.13 ±0.63	3.26	2.41	>50
24		1.04 ±0.06	3.25	2.73	>50
25		1.44 ±0.1	2.87	2.97	22
26	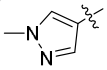	5.6 ±0.63[b]	2.99	2.26	>50
27		5.96 ±0.13	2.91	2.31	>50

[a] EC_{50} values are mean ± SD; n = 4 measurements; All SEM values are within 25% unless otherwise noted. [b] SEM = 1.72; [c] Calculated partition coefficient;[29] [d] (LLE = pEC_{50} – clogP)

As another important step in our preliminary hit-to-lead optimization of **1**, we have prepared a number of analogs to identify the optimal growth vectors for improving upon the *T. brucei* potency for this scaffold (**Table 4**). These studies have demonstrated that relocation of the aryl substituent from the C6 position of the 1,2-dihydroquinazolin-2-one scaffold to the C5 or C7

position significantly reduces *T. brucei* activity in this series. Although large, lipophilic substituents at the C7 (R^1) position can partially restore activity (e.g., compounds **31** and **32**), these compounds have low LLE values. Thus, our efforts to optimize this series have focused on using the C6 growth vector for optimizing the left-hand side of the scaffold.

Table 4. Effect of C5 (R^2) and C7 (R^1) substituents on 1,2-Dihydroquinazolin-2-one scaffold on *T. brucei* growth inhibition and MRC5 cytotoxicity

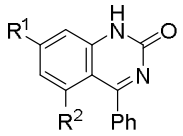

Cmpd.	R^1	R^2	*T. brucei* EC_{50} (μM)[a]	cLogP[b]	*T. brucei* LLE[c]	MRC5 (μM)
28		H	14.18 ±0.67	3.35	1.5	>50
29		H	>40	3.35	--	>50
30		H	>40	2.64	--	>50
31	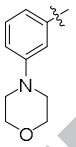	H	4.87 ±0.815	4.45	0.86	>50
32	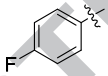	H	4.65 ±0.88	4.71	0.63	>50
33	H		>40	2.91	--	>50
34	H	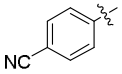	>40	4.42	--	>50

[a] EC_{50} values are mean ± SD; n = 4 measurements; All SEM values are within 25%.
[b] Calculated partition coefficient;[29] [c](LLE = pEC_{50} – clogP)

In preliminary efforts to improve aqueous solubility in this series, we have briefly explored strategies for increasing the overall fraction of sp^3 character (Fsp^3) in our molecules (**Table 5**), which has been shown to correlate with improved physical properties and clinical development potential.[27] Replacement of the C6 phenyl group with a methyl group (compound **35**) improves aqueous solubility, but with complete loss of *T. brucei* activity. Likewise, insertion of saturated heterocyclic groups at the C6 position on the 1,2-dihydroquinazolin-2-ones scaffold (compounds

36 - **38**) significantly improves aqueous solubility but also eliminates or reduces compound potency in our *T. brucei* assays.

Table 5. Effect of C4 and C6 alkyl, heteroalkyl, and substituted aromatic analogs on *T. brucei* growth inhibition, kinetic aqueous solubility, and MRC5 cytotoxicity

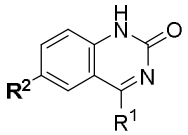

Cmpd.	R^1	R^2	*T. brucei* EC_{50} (μM)[a]	clogP[b]	*T. brucei* LLE[c]	Aq. Sol. (μM)[d]	MRC5 (μM)
35	Ph	CH_3	>40	3.43	--	80	>50
36	Ph	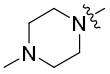	>40	2.87	--	>1000	>50
37	Ph	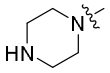	>20	2.38	--	>1000	>25
38	Ph		14.1 ±0.37	2.81	2.05	324	>50
39			3.14 ±0.28	3.77	1.74	13	>50
40	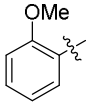		28.99 ±6.82	3.10	1.44	N.D.	>50
41		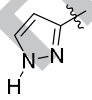	5.76 ±0.71	3.47	1.77	5	>50
42			5.95 ±1.45	2.58	2.65	74	>50

[a] EC_{50} values are mean ± SD; n = 4 measurements; All SEM values are within 25%.
[b] Calculated partition coefficient;[29] [c](LLE = pEC_{50} – clogP); [d]Kinetic aqueous solubility measured using chemiluminescent nitrogen detection (CLND) method.

Alternate C4 groups have also been explored with the goal of reducing the overall planarity of the system using either *ortho*-substituted phenyl or cycloalkyl groups (compounds **39** – **42**). The C4 cyclobutyl analog **42** produced the best solubility improvement in this series (aqueous solubility = 74 μM), albeit with a nearly 6-fold loss of potency in the *T. brucei* assay relative to the C4-phenyl analog **24**. Notably, due to the improved lipophilicity of **42** (cLogP = 2.58; $LogD_{7.4}$ =2.3), its efficiency (LLE = 2.65) approaches that of pyrazole **24** (LLE = 2.73). Taken together,

these studies suggest that maintaining an aromatic heterocycle such as the pyrazole at the C6 position may be crucial for achieving potent activity in the *T. brucei* assay for this series. However, insertion of small cycloalkyl groups such as cyclobutyl at the C4 position allows for improving aqueous solubility without significant loss of *T. brucei* activity. Based on these outcomes, future efforts will focus on appending additional polar or ionizable groups to the scaffold of **24** or **42** to further improve potency and solubility while maximizing LLE.

In an effort to identify additional applications for our novel 1,2-dihydroquinazolin-2-ones in the treatment of other neglected tropical diseases, we have also screened all new compounds in this series against *T. cruzi* and *L. donovani* (**Table 6**). Many proteins are highly conserved among *T. brucei*, *T. cruzi,* and *Leishmania sp.*,[28] so effective inhibitors against one trypanosomatid species could potentially aid in identifying new drug leads against other species. Several compounds in the series (compound **8, 9, 12, 13, 15, 16, 17, 21, 25, 39**) yield *T. cruzi* EC_{50} values below 10 μM, with all of these compounds demonstrating modest selectivity for *T. brucei* over *T. cruzi*. To date, pyrazole **39** is the most potent *T. cruzi* cell proliferation inhibitor (EC_{50} = 5.28 μM) in this series. No compounds in this 1,2-dihydroquinazolin-2-one series have shown significant activity in the *L. donovani* intracellular proliferation assay. As part of our ongoing effort to optimize new lead compounds in this series against *T. brucei*, we will continue to screen against *T. cruzi* and *L. donovani*, as well as relevant human cell lines to assess selectivity.

Table 6. Compared activities of generated analogs on kinetoplastid parasites growth inhibition and mammalian cell lines.

Cmpd.	*T. brucei* EC_{50} (μM)[a]	MRC5 EC_{50} (μM)	*T. cruzi* EC_{50} (μM)[a]	L6 EC_{50} (μM)[a]	*L. donovani* EC_{50} (μM)[a]	THP-1 EC_{50} (μM)[a]	*T. brucei* LLE	*T. cruzi* LLE	*L.d.* LLE
1	1.89 ±0.09	>50	10.94 ±2.65	>50	>5		2.38	1.62	1.96
5	5.32 ±0.8	> 50	16.84 ±2.26	>50	>5	> 50	1.8	1.3	1.82
6	5.35 ±0.5	> 50	15.84 ±0.54	>50	>5	> 50	1.93	1.45	1.96
7	5.29 ±0.66	> 50	14.85 ±1.45	>50	>5	> 50	1.8	1.35	1.82
8	5.07 ±0.05	> 50	8.94 ±1.91	>50	>5	> 50	1.44	1.19	1.44
9	5.24 ±0.23	> 50	9.56 ±1.41	>50	>5	> 50	1.42	1.16	1.44
10	5.21 ±0.18	> 50	18.42 ±1.52	> 50	>5	> 50	0.67	0.13	0.69
11	2.04 ±0.19	> 50	13.97 ±0.73	50	>5	> 50	1.64	0.81	1.25
12	1.77 ±0.08	> 50	6.29 ±0.62	> 50	>5	> 50	1.3	0.75	0.85
13	1.73 ±0.11	> 50	7.19 ±0.38	> 16	>5	> 50	1.04	0.42	0.58
14	4.88 ±0.58	> 50	> 20	> 50	>5	> 50	0.75	0.14	0.74
15	3.71 ±0.55	> 50	8.63 ±0.63	55.82 ±5.22	>5	50	0.72	0.36	0.59
16	4.29 ±0.29	> 50	9.48 ±1.59	23.03	>5	> 50	0.66	0.32	0.59
17	3.88 ±0.25	> 50	8.73 ±0.64	50	>5	> 50	0.71	0.35	0.59
18	1.71 ±0.17	> 50	17.41 ±1.71	> 50	>5	> 50	1.35	0.34	0.88
19	5.7 ±0.45	> 50	> 20	> 50	>5	> 50	1.61	0.66	1.66
20	5.17 ±0.26	> 50	15.06 ±1.01	> 50	>5	> 50	0.83	0.37	0.85
21	2.17 ±0.37	23.76	8.3 ±0.33	22.73 ±4.08	>5	> 50	1.21	0.63	0.85
22	10.04 ±2.95	> 50	> 20	> 50	>5	> 50	2.36	2.06	2.66

23	2.13 ±0.63	> 50	11.91 ±0.84	> 50	>5	> 50	2.41	1.67	2.04
24	1.04 ±0.06	> 50	13.33 ±0.82	>50	>5	> 50	2.73	1.62	2.05
25	1.44 ±0.1	22	8.33 ±1.67	> 50	>5	> 50	2.97	2.21	2.43
26	5.6 ±0.63	> 50	> 20	>50	>5	> 50	2.26	1.71	
27	5.96 ±0.13	> 50	17.42 ±0.72	> 50	>5	> 50	2.31	1.85	2.39
28	14.18 ±0.67	> 50	> 20		>5	> 50	1.5	1.35	1.96
29	> 40	> 50	> 20	7.73 ±0.72	>5	> 50	1.05	1.35	1.96
30	> 40	> 50	> 20		>5	> 50	1.76	2.06	2.66
31	4.87 ±0.815	> 50	> 20	4.53 ±0.2	>5	> 50	0.86	0.25	0.85
32	4.65 ±0.88	> 50	> 20		>5	> 50	0.63	-0.01	0.59
33	> 40	> 50	> 20	> 50	>5	> 50	1.49	1.79	2.39
34	> 40	> 50	> 20	> 50	>5	> 50	-0.02	0.28	0.88
35	> 40	> 50	> 20	> 50	>5	> 50	0.97	1.27	1.87
36	> 40	> 50	> 20	> 50	>5	> 50	1.53	1.83	2.43
37	> 20	> 25	> 10	> 25	> 2.5	> 25	2.01	2.31	2.92
38	14.1 ±0.37	> 50	> 20	> 50	>5	> 50	2.05	1.89	2.5
39	3.14 ±0.28	> 50	5.28 ±0.23	> 50	>5	> 50	1.74	1.51	1.53
40	28.99 ±6.82	> 50	20	> 50	>5	> 50	1.44	1.6	2.21
41	5.76 ±0.71	> 50	20	> 50	>5	> 50	1.77	1.23	1.84
42	5.95 ±1.45	> 50	16.89 ±3.27	> 50	>5	> 50	2.65	2.2	2.72

[a] EC_{50} values are mean ± SD; n = 4 measurements; All SEM values are within 25%.

In summary, through our compound synthesis and SAR studies, we have confirmed the previously reported activity of **1** (NEU-0001101) in a *T. brucei* cell proliferation assay and have demonstrated that this hit can be modified to replace the pyridine ring, a potential drug safety liability. Through the synthesis of a number of C5-, C6-, and C7-substituted analogs, we have also shown that the C6 position presents the best growth vector for further elaboration of this scaffold. Furthermore, we have shown that replacement of the pyridine with a pyrazole ring (Compound **24**) improves potency, lipophilicity, and LLE relative to the original hit, while maintaining good in vitro metabolic stability. Additionally, placement of the cyclobutyl at the C4 position (Compound **42**) has improved aqueous solubility without dramatic loss of *T. brucei* activity. Based on these outcomes, our ongoing hit-to-lead optimization studies are exploring additional modifications of the C6 pyrazole and C4 cyclobutyl groups to further improve potency and solubility while maximizing LLE.

Acknowledgements

We thank Michael P. Pollastri and Lori Ferrins at Northeastern University for compound logistics and data management support and manuscript editing suggestions; AstraZeneca for performing in vitro ADME assays; Tanya Cervantes for LC-MS and NMR technical support. Funding was provided by the Boettcher Foundation's Webb-Waring Biomedical Research Program, Boettcher Collaboration Grant, Research Corporation Cottrell College Science Award, and NSF-MRI CHE-1429567. Biological assays were funded by the National Institute of Allergy and Infectious Diseases (MPP and MN, R01AI114685), Spanish Ministerio de Economía, Industria y Competitividad, (SAF2015-71444-P for MN, SAF2015-68042-R for FG and SAF2016-79957-R for DG-P), Junta de Andalucía (FG, CTS-7282) and Subdirección General de Redes y Centros de Investigación Cooperativa (RICET) (MN RD16/0027/0019, DG-P RD16/0027/0014).

References and Notes

1. World Health Organization. Trypanosomiasis, Human African (Sleeping Sickness); http://www.who.int/mediacentre/factsheets/fs259/en/; Accessed 28.04.17.

2. Kuepfer I, Schmid C, Allan M, Edielu A, Haary EP, Kakembo A, Kibona S, Blum J, Burri C. Safety and Efficacy of the 10-Day Melarsoprol Schedule for the Treatment of Second Stage Rhodesiense Sleeping Sickness. *PLOS Neglected Trop Dis.* 2012;6:e1695.

3. Schmid C, Richer M, Bilenge CMM, Josenando T, Chappuis F, Manthelot CR, Nangouma A, Doua F, Asumu PN, Simarro PP, Burri C. Effectiveness of a 10-Day Melarsoprol Schedule for

the Treatment of Late-Stage Human African Trypanosomiasis: Confirmation from a Multinational Study (Impamel II). *J Infect Dis.* 2005;191:1922–1931.

4. Baker N, de Koning HP, Mäser P, Horn D, Drug Resistance in African Trypanosomiasis: The Melarsoprol and Pentamidine Story. *Trends in Parasitology.* 2013;29:110–118.

5. World Health Organization. Human African Trypanosomiasis: Research http://www.who.int/trypanosomiasis_african/research/en/; Accessed 28.04.17.

6. Gjini E. Human African Trypanosomiasis: What Are the Prospects for Control? *Human Parasitic Diseases*. 2017;9:1–10.

7. Diaz R, Luengo-Arratta SA, Seixas JD, Amata E, Devine W, Cordon-Obras C, Rojas-Barros DI, Jimenez E, Ortega F, Crouch S, Colmenarejo G, Fiandor JM, Martin JJ, Berlanga M, Gonzalez S, Manzano P, Navarro M, Pollastri MP. Identification and Characterization of Hundreds of Potent and Selective Inhibitors of Trypanosoma Brucei Growth from a Kinase-Targeted Library Screening Campaign. *PLoS Neglected Trop Dis.* 2014;8:e3253.

8. Wager TT, Chandrasekaran RY, Hou X, Troutman MD, Verhoest PR, Villalobos A, Will Y. Defining Desirable Central Nervous System Drug Space through the Alignment of Molecular Properties, in Vitro ADME, and Safety Attributes. *ACS Chem Neurosci.* 2010;1: 420-434.

9. Wager TT, Hou X, Verhoest PR, Villalobos A. Moving beyond Rules: The Development of a Central Nervous System Multiparameter Optimization (CNS MPO) Approach to Enable Alignment of Druglike Properties. *ACS Chem Neurosci.* 2010;1:435-449.

10. Hitchcock SA, Pennington LD. Structure–Brain Exposure Relationships. *J Med Chem.* 2006; 49:7559–7583.

11. LE = 1.4(-*log*EC_{50})/#Heavy atoms)

12. Hopkins AL, Groom CR, Alex A. Ligand Efficiency: A Useful Metric for Lead Selection. *Drug Discovery Today.* 2004;9:430–431.

13. Hopkins AL, Keserü GM, Leeson PD, Rees DC, Reynolds CH. The Role of Ligand Efficiency Metrics in Drug Discovery. *Nat Rev Drug Discov.* 2014; 13:105–121.

14. Bergman J, Brynwolf A, Elman B, Vuorinen E. Synthesis of Quinazolines. *Tetrahedron*. 1986; 42:3697-3706.

15. Suzuki coupling protocol was adapted from Adams ND, Darcy MG, Dhanak D, Duffy KJ, Fitch DM, Knight SD, Newlander KA, Shaw AN. *PCT Int. Appl.* 2006; WO 2006113432.

16. Rankovic Z, Jamieson C, Morphy R. High Throughput Screening Approach to Lead Discovery. In: Rankovic Z, Morphy R., eds. *Lead Generation Approaches in Drug Discovery*. Hoboken, NJ: John Wiley & Sons Inc:, 2010:21–71.

17. Frearson JA, Collie IT. HTS and Hit Finding in Academia – from Chemical Genomics to Drug Discovery. *Drug Discovery Today*. 2009;14:1150–1158.

18. Dahlin JL, Nissink JWM, Strasser JM, Francis S, Higgins L, Zhou H, Zhang Z, Walters MA. PAINS in the Assay: Chemical Mechanisms of Assay Interference and Promiscuous Enzymatic Inhibition Observed during a Sulfhydryl-Scavenging HTS. *J Med Chem.* 2015; 58:2091–2113.

19. Kaul KL, Novak RF. Inhibition and Induction of Rabbit Liver Microsomal Cytochrome P-450 by Pyridine. *J Pharmacol Exp Ther*. 1987; 243:384–390.

20. Edwards MP, Price DA. Role of Physicochemical Properties and Ligand Lipophilicity Efficiency in Addressing Drug Safety Risks. In: Macor JE. ed. *Annual Reports in Medicinal Chemistry, Vol. 45.* New York, NY: Academic Press; 2010:380–391.

21. Perola E. An Analysis of the Binding Efficiencies of Drugs and Their Leads in Successful Drug Discovery Programs. *J Med Chem.* 2010;53:2986–2997.

22. Gleeson MP, Hersey A, Montanari D, Overington J. Probing the Links between in Vitro Potency, ADMET and Physicochemical Parameters. *Nat Rev Drug Discov.* 2011;10:197–208.

23. Hughes JD, Blagg J, Price DA, Bailey S, DeCrescenzo GA, Devraj RV, Ellsworth E, Fobian YM, Gibbs ME, Gilles RW, Greene N, Huang E, Krieger-Burke T, Loesel J, Wager T, Whiteley L, Zhang Y. Physiochemical Drug Properties Associated with in Vivo Toxicological Outcomes. *Bioorg Med Chem Lett* 2008;18:4872–4875.

24. Johnson TW, Dress KR, Edwards M. Using the Golden Triangle to Optimize Clearance and Oral Absorption. *Bioorg Med Chem Lett.* 2009;19:5560–5564.

25. Waring MJ. Defining Optimum Lipophilicity and Molecular Weight Ranges for Drug candidates—Molecular Weight Dependent Lower Log D Limits Based on Permeability. *Bioorg Med Chem Lett* 2009; 19:2844–2851.

26. Waring MJ, Johnstone CA. Quantitative Assessment of hERG Liability as a Function of Lipophilicity. *Bioorg Med Chem Lett.* 2007; 17:1759–1764.

27. Lovering F, Bikker J, Humblet C. Escape from Flatland: Increasing Saturation as an Approach to Improving Clinical Success. *J Med Chem.* 2009;52:6752–6756.

28. Merritt C, Silva LE, Tanner AL, Stuart K, Pollastri MP. Kinases as Druggable Targets in Trypanosomatid Protozoan Parasites. *Chem Rev.* 2014; 114:11280–11304.

29. Calculator Plugins were used for cLogP calculation, ChemAxon (http://www.chemaxon.com).

GRAPHICAL ABSTRACT

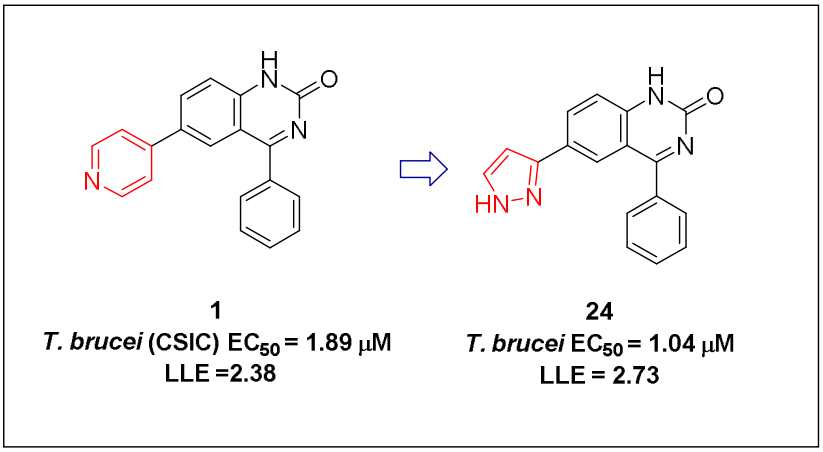

1
T. brucei (CSIC) EC_{50} = 1.89 μM
LLE =2.38

24
T. brucei EC_{50} = 1.04 μM
LLE = 2.73